



Liraglutide prevents β -cell apoptosis via inactivation of NOX2 and its related signaling pathway



Min Ding¹, Qian-Hua Fang¹, Yuan-Tao Cui, Qi-Ling Shen, Qian Liu, Peng-Hua Wang, De-Min Yu^{*}, Chun-Jun Li^{*}

NHC Key Laboratory of Hormones and Development (Tianjin Medical University), Tianjin Key Laboratory of Metabolic Diseases, Tianjin Medical University Metabolic Diseases Hospital & Tianjin Institute of Endocrinology, Tianjin 300070, PR China

ARTICLE INFO

Article history:

Received 30 October 2018
Received in revised form 20 November 2018
Accepted 26 December 2018
Available online 2 January 2019

Keywords:

Apoptosis
Liraglutide
GLP-1
NOX2
 β -Cells

ABSTRACT

Aims: High glucose (HG)-induced pancreatic β -cell apoptosis may be a major contributor to the progression of diabetes mellitus (DM). NADPH oxidase (NOX2) has been considered a crucial regulator in β -cell apoptosis. This study was designed to evaluate the impact of GLP-1 receptor agonist (GLP-1Ra) liraglutide on pancreatic β -cell apoptosis in diabetes and the underlying mechanisms involved.

Methods: The diabetic rat models induced by streptozotocin (STZ) and a high fat diet (HFD) received 12 weeks of liraglutide treatment. Hyperglycemic clamp test was carried out to evaluate β -cell function in vivo. Flow cytometry analysis was used to measure apoptosis rates in vitro. DCFH-DA method was used to detect ROS level in vivo and in vitro.

Results: Liraglutide significantly improved islet function and morphology in diabetic rats and decreased cell apoptosis rates. Thr183/Thr185 p-JNK1/2 and NOX2 levels reduced in diabetic rats and HG-induced INS-1 cell following liraglutide treatment. In addition, liraglutide upregulated the phosphorylation of AMPK α (p-AMPK α), which prevented NOX2 activation and alleviated HG-induced β -cell apoptosis.

Conclusion: The p-AMPK α /NOX2/JNK1/2 pathway is essential for liraglutide to attenuate HG-induced β -cell apoptosis, which further proves that GLP-1Ras may become promising therapeutics for diabetes mellitus.

© 2019 The Authors. This is an open access article under the CC BY-NC-ND license (<http://creativecommons.org/licenses/by-nc-nd/4.0/>).

1. Introduction

Impairments in pancreatic β -cell insulin secretion are a hallmark of the progression of type 2 diabetes (T2DM). It has been clearly reported that β -cell dysfunction and impaired insulin secretion are key contributors to chronic hyperglycemia in T2DM patients, instead of primarily being driven by insulin resistance.¹ T2DM patients often show persistent deteriorated hyperglycemia, which triggers the development of the late complications of diabetes and progressive deterioration of β -cell masses as well as the lack of insulin synthesis.^{2–}

Secreted from intestinal L cells, Glucagon like peptide-1 (GLP-1) as an incretin hormone stimulated glucose-dependent insulin secretion in β -cells.³ GLP-1 exerts several beneficial effects to improve diabetes mellitus (DM). First, GLP-1 promoted the expression of glucose transporter 2, which plays a pivotal role in glucose movement across the cell membrane, in pancreatic β -cells.⁴ Furthermore, GLP-1 induced

insulin secretion from pancreatic β -cells and repressed glucagon secretion from pancreatic α -cells.⁵ In addition, GLP-1 led to a decrease in the secretion of proinflammatory cytokines, such as tumor necrosis factor α (TNF α), interleukin β (IL- β), and inducible nitric oxide synthase (iNOS).⁶ Therefore, GLP-1 restores pancreatic β -cell masses and insulin sensitivity. A clinical study revealed that GLP-1 receptor agonist (GLP-1Ra) partially restored the first-phase insulin secretion in subjects with established T2DM.⁷ Improving insulin sensitivity and β -cell function, six-week courses of GLP-1Ra significantly decreased the concentrations of plasma glucose in patients with T2DM.⁸ Interestingly, recent studies have shown that GLP-1Ra prevented β -cell apoptosis in diabetic mice as well as cytokine-treated rat islets in vitro.⁹ Although the mechanism of how GLP-1 inhibits β -cell apoptosis and prevents DM progression has been explored extensively, its detailed mechanisms still remain to be explored.

Brownlee M proposed a pathogenesis theory that there were five mechanisms associated with tissue damage, including the polyol pathway, increased formation of advanced glycation end products (AGEs), hyperglycemia-induced activation of protein kinase C (PKC) isoforms, increased hexosamine pathway flux and the consequent over modification of proteins by N-acetylglucosamine.¹⁰ The activation of the above mechanisms all resulted from the overexpression of reactive oxygen

Conflict of Interest Statement: The authors declare that they have no conflicts of interests.

^{*} Corresponding authors.

E-mail addresses: yudemintj@126.com (D.-M. Yu), li_chunjun@126.com (C.-J. Li).

¹ Min Ding and Qian-Hua Fang contributed equally to this study.

species (ROS) in mitochondria.¹¹ In addition, β -cells exposed to chronic hyperglycemia also generated ROS and reactive nitrogen species (RNS), which would accelerate the disease progression and further β -cell loss.¹² The nicotinamide adenine dinucleotide phosphate oxidases (NOX) family is one of the main sources of superoxide radical formation in many cell types, including β -cells.¹³ Because reactive oxygen species are involved in intracellular signaling, phagocyte-like NADPH oxidase activation by glucose may play an important role for beta-cell functioning.¹⁴

Nicotinamide adenine dinucleotide phosphate oxidases 2 (NOX2) as a critical subunit of NOX is associated with the occurrence of multiple diseases. An interesting study revealed that the endothelial and vascular functions of human carriers of hereditary NOX2 deficiency were better than those of healthy subjects.¹⁵ In addition, atherosclerotic plaque formation in ApoE^{-/-} mice would be mitigated because NOX2 knockout led to an increased NO bioavailability and a significant reduction in aortic ROS production. These experiments indicate that inhibiting NOX2 generation plays a protective effect on human atherosclerosis. Inhibiting NOX2 activity could help reduce kidney damage via the inhibition of apoptosis in a C57BL/6J mouse model.¹⁶ NOX2 was responsible for inflammatory bowel disease as result of the generation of peroxynitrite in murine nonalcoholic fatty liver disease.¹⁷ In addition, the role of NOX2 in diabetes also has been explored extensively. NOX2 deficiency preserved islet function via reductions in ROS, immune responses and β -cell apoptosis in STZ-induced diabetic mice, which indicates that NOX2 might be a new therapeutic target for the regulation of insulin secretion.¹⁸ The NOX-ROS-JNK1/2 signaling pathway led to increased oxidative stress and β -cell apoptosis in a high fat and glucose setting, and specific inhibition of the signaling pathway agent significantly decreased β -cell apoptosis.¹⁹ Notably, Balteau M reported that GLP-1 antagonized NOX2 activation induced by hyperglycemia in adult cardiomyocytes.²⁰ GLP-1Ra might keep β -cells from apoptosis to maintain the β -cell mass and its insulin secretory function via inhibition of the JNK and GSK3 β .²¹ Whether GLP-1 also inhibits NOX2 activation induced by hyperglycemia in β -cells remains unclear. Therefore, we hypothesized that the effect of GLP-1Ra on protecting β -cell apoptosis was associated with the inactivation of NOX2.

2. Materials and methods

2.1. Experimental animals

Thirty-six male Sprague Dawley (SD) rats, aged 8 weeks, were purchased from Beijing (HuaFuKang Biotechnology Co. LTD) and given standard rat chow and water ad libitum. The animals were allowed 1 week of acclimatization before being randomly divided into three groups. T2DM was induced by injecting freshly prepared streptozotocin (STZ, 30 mg/kg, i.p.; Sigma-Aldrich, St. Louis, MO, USA) in cold citrate buffer (0.1 M, pH 4.2) into overnight-fasted SD rats. Control rats were administered an intraperitoneal injection of acetate buffer. Some rats were put on a high-fat diet (HFD, D12492, Research Diets) for 8 weeks following the intraperitoneal injection of acetate buffer or STZ. Rats with 8-h fasting blood glucose levels >200 mg/dL were considered to be diabetic rodents. One week after the induction of diabetes, half of the diabetic rats were randomly selected and treated with subcutaneous injections of liraglutide for 12 weeks at doses of 0.2 mg/kg/24 h, as previously reported.²² An age-matched control group was included and fed regular rodent chow diet with free access to water. Animals were housed (5 rats/cage) under controlled ambient conditions following a 12:12-h light-dark cycle, with lights on at 6:00 AM. These studies were approved by the Animal Use Committee of Tianjin Medical University and were conducted in compliance with the Animal Use Guidelines of the University Committee.

2.2. Islet isolation

Rat islets were collected using a traditional collagenase digestion method. Rats were sacrificed by means of the broken heart method,

and collagenase (8–10 mL, 1 g/L) (Liberase human islet, Roche, Indianapolis, IN, USA) was injected through the liver pancreatic duct before a water bath for 17 min at 37 ± 1 °C. Rats were placed in an ice bath, to which 4 °C Hanks fluid was quickly added to approximately 40 to 50 mL to terminate the digestion. Wild swings in the pancreas to a sandy shape were observed. The tissue was kept in an ice bath for 10 min until static layering was noted. Then, for upper liquid absorption, 40–50 mL 4 °C Hanks fluid was added; this step was repeated twice. A stereomicroscope was used to manually identify the circular islet shapes before incubation in RPMI1640 medium. After isolation, the islets were cultured for 48 h for assay and experiment procedures. Then, proteins were extracted western blot analysis and media was collected for the insulin assay.²³

2.3. Hyperglycemic clamp

After the animals were fasted overnight and terminally anesthetized, the animals' left carotid artery and caudal vein were catheterized. Following an initial stabilization period (30 min), a hyperglycemic clamp was initiated with a priming dose of glucose (350 mg/kg; 1 min) administered into the caudal vein.²⁴ Then, a 25% glucose solution was infused through the venous catheter at a slow rate. The resulting blood glucose concentration was measured every 5–10 min to maintain levels at 5.5 mM above the fasting concentration by adjusting the glucose infusion rate. Arterial blood samples (2 mL) were taken at 0 min for the determination of insulin and glycosylated hemoglobin (HbA1c) levels measured by High Performance Liquid Chromatography. Arterial blood samples (400 μ L) were taken at 5, 10, 60, 90 and 120 min to determine the blood glucose and plasma insulin (Millipore-Linco EZRMI-13K) concentrations. Blood samples were centrifuged (15,700 \times g, 3–5 min, 4 °C) immediately for plasma separation. Each sample was stored at -80 °C for later analysis.

2.4. Histological and immunohistochemical analyses

For histopathological assessment, pancreatic sections were stained for hematoxylin and eosin (H&E) using methods that were described previously.²⁵ Immunohistochemical analysis on sections of the pancreas was undertaken as described previously.²⁶ To detect the β - and α -cells mass ratio and the NOX2, p-AMPK α , and p-JNK1/2 expression in each pancreas, tissue sections were incubated with anti-glucagon (Sigma-Aldrich, St. Louis, MO, USA), anti-insulin, anti-NOX2, anti-p-AMPK α (Cell signaling, Beverly, MA, USA), and anti-p-JNK1/2 antibody (Abcam, Cambridge, UK). Afterwards, sections were incubated with a secondary antibody (Zhongshan, Beijing, China) for 2 h at room temperature, and fluorescent images were captured with a confocal microscope (Olympus FV1000, Tokyo, Japan). Immunohistochemical images were captured with Image-Pro Plus software.

2.5. Cell culture

INS-1832/13 cells (kindly provided by Professor Daiqing Li, Department of Endocrinology, Metabolic Disease Hospital, Tianjin Medical University, China) were grown in RPMI-1640 medium containing 10% fetal bovine serum (FBS), 100 U/mL streptomycin, 100 U/mL penicillin, 10 mmol/L glutamine, 1 mmol/L sodium pyruvate, 10 mmol/L HEPES, and 50 μ M β -mercaptoethanol in an atmosphere of 5% CO₂ at 37 °C, and glucose was adjusted to 11.1 mM.

2.6. Apoptosis

Cellular apoptosis was measured as follows. 1) First, a TUNEL assay was completed for the detection of apoptotic cells in pancreas. Staining was performed in 7 μ m thick paraffin-embedded sections of pancreas with the "In Situ Cell Death Detection Kit" (TUNEL) (Roche Applied Science, #12156792910, Basel, Switzerland) according to manufacturer's

instructions. The signals were visualized under LEICA's DIM6000 confocal microscope. Quantification of the signals was performed using NIH ImageJ 1.49 software. β -cell apoptosis was quantified by the percentage of insulin+ and TUNEL+ double positive cells/insulin+ cells in the pancreases.²⁷ 2) Immunohistochemistry and western blot analysis with Cleaved Caspase3 (Asp175, #9661, Cell Signaling Technology; USA) antibodies; and 3) Annexin V-FITC and PI apoptosis detection kit (Roche companies, USA) followed by flow cytometry.

2.7. Flow cytometry analysis

Surface exposure of phosphatidyl serine in apoptotic cells was quantitatively detected using the Annexin V-FITC and PI apoptosis detection kit (Roche companies, USA). Briefly, cells were seeded into 6-well plates (1.0×10^6 cells/mL) and incubated for 24 h. Then, the medium was changed to 0.5% FBS-containing RPMI1640, and cells were starved for 12 h. Cells were incubated in the presence or absence of liraglutide (100 nmol/L) before being challenged with HG (30 mmol/L) for 48 h. Cells were divided into five groups: Normal control (N), HG, Mannitol (M), N + GLP-1Ra (G), and HG + G. After treatment with the H₂O₂ for varying times, cells were harvested and washed twice with ice-cold PBS. After 5 min of centrifuging at 5000 rpm, Annexin V-FITC and PI double staining were performed according to the manufacturer's instructions. Cell apoptosis was analyzed with AnnexinV-FITC/propidium iodide (PI) flow cytometry (Becton Dickinson, San Jose, CA, USA). Annexin V-FITC-positive, PI-negative cells were scored as apoptotic. Double-stained cells were considered either as necrotic or as late apoptotic. Immunohistochemical analysis of sections of the pancreas was undertaken as described previously.²⁸

2.8. Western blot analysis

The total protein (60 μ g) extracted from cardiac tissues was fractionated by SDS-PAGE (10% polyacrylamide gels) and transferred to a nitrocellulose membrane. The membrane was blocked with 5% nonfat milk for 1.5 h at room temperature. The membrane was then incubated with primary antibodies collagen I (1:800 dilution, Proteintech, China), collagen III (1:2000 dilution, Proteintech, China) and GAPDH (1:1000 dilution, Kangcheng Inc., China) on a shaking bed overnight at 4 °C. The membrane was then washed with PBST 3 times and incubated with secondary antibodies for 1 h at room temperature. Finally, the membranes were rinsed with PBST before being scanned by Imaging System (LI-COR Biosciences, Lincoln, NE, USA). Whole cell lysates were prepared by lysis cells in a Proprep-protein extraction solution (Intron Biotechnology, Seoul, Korea) containing 10 mM sodium phosphate (pH 7), 1% Triton X-100, 0.1% SDS, 2 mM EDTA, 150 mM NaCl, 50 mM NaF, 0.1 mM sodium vanadate, 4 μ g/mL leupeptin, 1 mM PMSF, and protein concentration of the lysates were measured with a Bio-Rad protein assay kit (Bio-Rad, Hercules, CA, USA). Equal amounts of proteins (20 μ g) were separated on a 4–20% SDS-PAGE and transferred by electroblotting to a nitrocellulose membrane. The membranes were washed with PBST containing 5% nonfat dry milk at room temperature and incubated for 2 h with the primary antibodies under the same conditions. The following primary antibodies were used: anti-JNK, anti-Thr183/Tyr185 phospho-JNK1/2, anti-phospho-AMPK α (Cell Signaling, Beverly, MA, USA), anti-Caspase3 (Cell Signaling, Beverly, MA, USA), and anti- β -actin (for internal control) (Sigma, St. Louis, MO, USA). The membranes were washed in PBST and incubated for 1 h with horseradish peroxidase-conjugated sheep anti-mouse and donkey anti-rabbit immunoglobulin antibody (1:500) (Amersham Pharmacia Biotechnology, Tokyo, Japan) under the same conditions. After washing with PBST, the specific signals were detected with an enhanced chemiluminescence detection system (Amersham Pharmacia Biotechnology, Tokyo, Japan). Reagents for electrophoresis were obtained from Bio-Rad Laboratories (Hercules, CA, USA).

2.9. Measurement of ROS level in islets and INS-1 cells

ROS levels were measured by the DCFH-DA method. DCFH-DA is a non-fluorescent compound, and it can be enzymatically converted to a highly fluorescent compound, DCF, in the presence of ROS. In brief, islets were extracted by a traditional collagenase digestion method, and ROS levels were quantitated by the DCFH-DA method. Islets were incubated for 15 min in a 500 μ L RPMI1640 solution containing 2.5 μ mol/L DCFH-DA with or without pretreated with 100 μ mol/L Apocynin, a specific NOX2 inhibitor (Sigma-Aldrich, St. Louis, MO), 3 h in a 37 °C thermostat. In vitro, INS-1 cells were washed with PBS and incubated with DCFH-DA at a 10 μ mol/L final concentration for 30 min at 37 °C in darkness. For the inhibition studies, 100 μ g/mL Apocynin was added to the medium with or without GLP-1Ra treatment. The fluorescence intensity was measured in the microplate reader (Spectra MAX, Gemini EM, Molecular Device) at an excitation wave length of 485 nm and an emission wave length of 538 nm after the cells were washed three times with PBS to remove the extracellular DCFH-DA. The level of intracellular ROS was shown as a percentage of the non-treated control. The results were analyzed with the Image-Pro Plus 6.0 image analysis system.

2.10. Statistical analysis

All values are presented as the mean \pm SEM. Significant differences between 3 groups were determined using one-way analysis of variance followed by the LSD test. Paired *t*-tests were used to assess normally distributed data between individuals at before and after treatment (pre-post). The SPSS statistical software package (Version 17.0, Chicago, IL, USA) was used for the statistical analysis, and a *P* value <0.05 was considered to be statistically significant.

3. Results

3.1. Effects of liraglutide on general characteristics in STZ/HFD-induced diabetic rats

As shown in Fig. 1A, the body weight of the rats on the STZ/HFD challenge were significantly higher than those of the rats fed a chow diet from 0 to 5 weeks. From 5 to 12 weeks, the rats in the DM group and liraglutide (0.2 mg/kg/24 h) group shown decreased body weight compared to the control rats. Over time, the body weight in control rats had a slight increase, while there were no significant differences between the DM group and the liraglutide group (Fig. 1A). Food intake (kcal/kg/h) was higher in the DM group than in the control group, which was higher than in the liraglutide group. Significant differences among the three groups were observed ($F = 46.766$, $P = 0.000$) (Fig. 1B). As shown in Fig. 1C, the average blood glucose levels showed no significant differences between the T2DM group and the liraglutide group (19.29 ± 2.54 vs. 21.31 ± 1.52 mmol/L, $P = 0.087$). The average blood glucose in rats was calculated every two weeks, and the blood glucose levels of the three groups showed significant differences ($F = 11.606$, $P = 0.005$). Liraglutide treatment significantly reduced the blood glucose levels of diabetic rats ($F = 54.069$, $P = 0.006$). Similarly, 12 weeks of liraglutide treatment obviously reduced the HbA1c levels of diabetic rats (8.1 ± 0.3 vs. $6.9 \pm 0.4\%$), while these levels were still slightly higher than those of the control group (Fig. 1D, $F = 45.420$, $P = 0.000$).

3.2. Effects of liraglutide on pancreatic islet function and morphology

A hyperglycemic clamp experiment was carried out in order to determine the effects of liraglutide on the STZ/HFD-induced diabetic rats. Liraglutide treatment improved the reduced glucose infusion rate (GIR) in the T2DM group, which was significantly lower than that in the normal group, displayed an increase in insulin secretion (Fig. 2A–B). The first- and second-phase of β -cells secretion decreased obviously

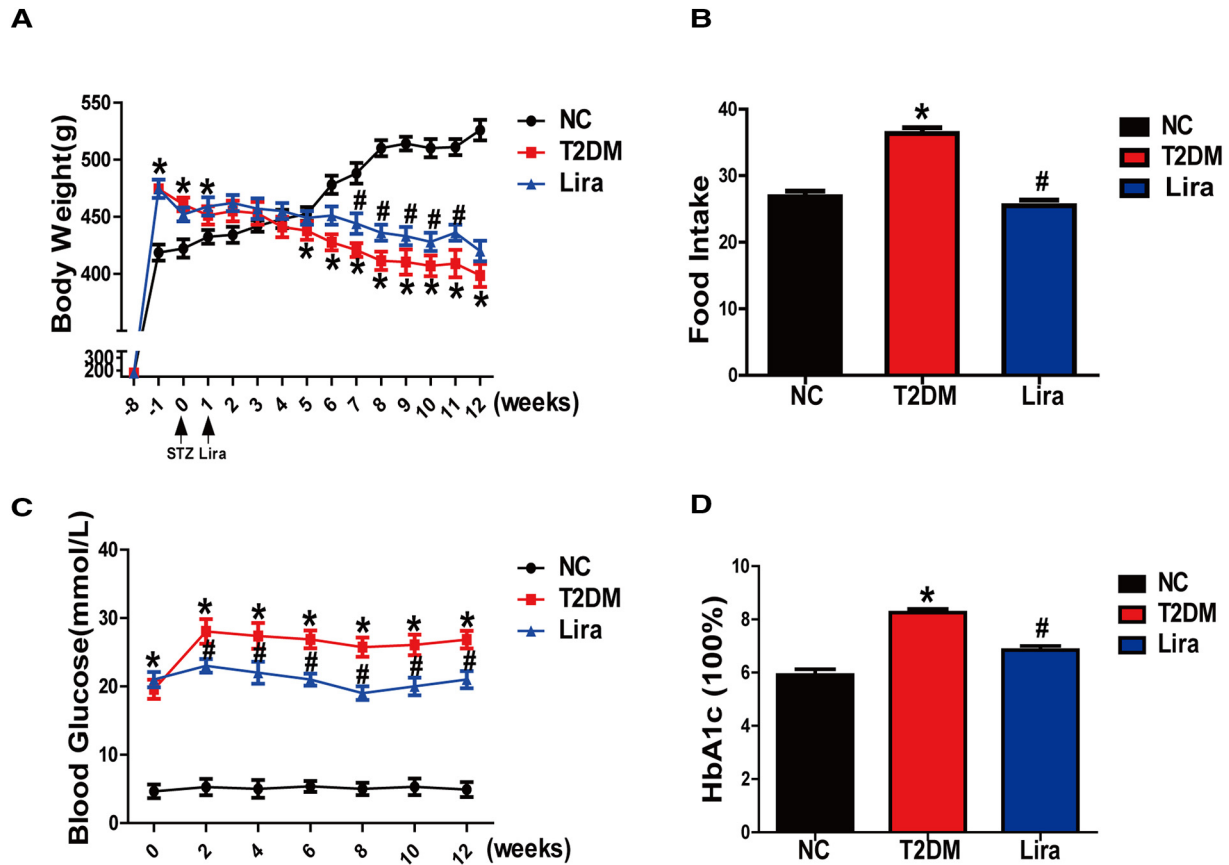


Fig. 1. Effects of liraglutide on general characteristics of STZ/HFD-induced diabetic rats.

in the T2DM group but improved over the period of liraglutide administration. The first- and second-phase plasma insulin concentrations in the liraglutide group were markedly increased compared with those in the T2DM group ($P = 0.004$) but were still lower than those in the control group ($P = 0.000$) (Fig. 2C). Islet morphology was assessed by HE staining and with insulin and glucagon immunofluorescent double-stained sections. Compared with the normal group, the diabetic group showed abnormal islet morphology, as evidenced by a disarray of the islet architecture and irregular islet boundaries. However, 12 weeks of liraglutide treatment partially restored the above morbid islet morphology (Fig. 2D). Pancreatic islets from normal rats outnumber those from diabetic rats, as demonstrated by insulin-positive β -cells (green) in the core region and glucagon-positive α -cells (red) in the peripheral region (Fig. 2E). At least 20 images per animal were captured, and the ratio of α/β was calculated with a gray value of glucagon/insulin using Image-Pro-Plus 6.0 (Media cybernetics, USA). The average glucagon and insulin fluorescent gray ratio increased in the T2DM group significantly compared to that in the control group ($P = 0.000$) and decreased following the 12-week liraglutide treatment ($P = 0.002$) (Fig. 2F).

3.3. Liraglutide suppresses HG-induced β -cell apoptosis in rats and INS-1 cells

To confirm whether GLP-1Ra could suppresses the high glucose (HG)-induced β -cell apoptosis, immunohistochemistry (IHC) and TUNEL staining were performed in the pancreatic sections from different groups. Western blot and Annexin V-FITC/PI flow cytometry were used to evaluate the Cleaved Caspase 3 and Caspase 3 expression levels and the INS-1 cell apoptosis rates, respectively. Liraglutide inhibited the increased Cleaved Caspase 3 in the islets from diabetic rats compared with normal rats (Fig. 3A). Compared with normal group, the increased pancreatic apoptosis in T2DM rats indicated by positive TUNEL staining

showed by red arrows was improved after liraglutide treatment (Fig. 3B). Liraglutide blocked the HG-induced Cleaved Caspase 3 activation in pancreatic islets (Fig. 3C $P < 0.05$). Then we detected the impact of HG (30 mmol/L) on INS-1 cell in vitro experiments. Our data demonstrated that the apoptosis rate caused by HG increased by 7.44 folds in INS-1 cells (N vs. HG, $P = 0.000$), becoming significantly higher than that in the mannitol isotonic (30 mmol/L) group (M vs. HG, $P = 0.000$). However, HG-induced apoptosis was reduced by 63.1% when cells were incubated in the presence of liraglutide (100 nmol/L) (Fig. 3D $P = 0.000$). The Cleaved Caspase 3/Caspase 3 levels in INS-1 cells showed the same tendency following treatment with liraglutide (Fig. 3E $P = 0.000$). Before the experiments, INS-1 cells at 80% confluence were cultured for 24 h in 11.1 mmol/L glucose-containing RPMI1640 medium, and cells were then incubated in the presence or absence of liraglutide before being challenged with HG (30 mmol/L) for 48 h.

3.4. Liraglutide prevents HG-mediated β -cell apoptosis by inhibiting NOX2-derived ROS generation

Reactive oxygen species (ROS) are the main products of oxidative stress in cells when they encounter stressful stimuli. Moreover, an overaccumulation of ROS has detrimental effects on general homeostasis.²⁹ ROS levels were significantly increased by 5.7 folds and 7.4 folds in INS-1 cells exposed to mannitol and HG (30 mmol/L) compared with the control group, respectively. Pre-treatment with liraglutide and Apocynin could both mitigate cells ROS levels in INS-1 cells cultured in HG (Fig. 4A). To our surprise, although the joint application of liraglutide and Apocynin also alleviated ROS levels, there was no statistical difference in cell apoptosis rates among HG + G, HG + A and HG + A + G group (Fig. 4A). Available research has revealed that NOX2 was a major source of ROS in pancreatic β -cells in the setting of

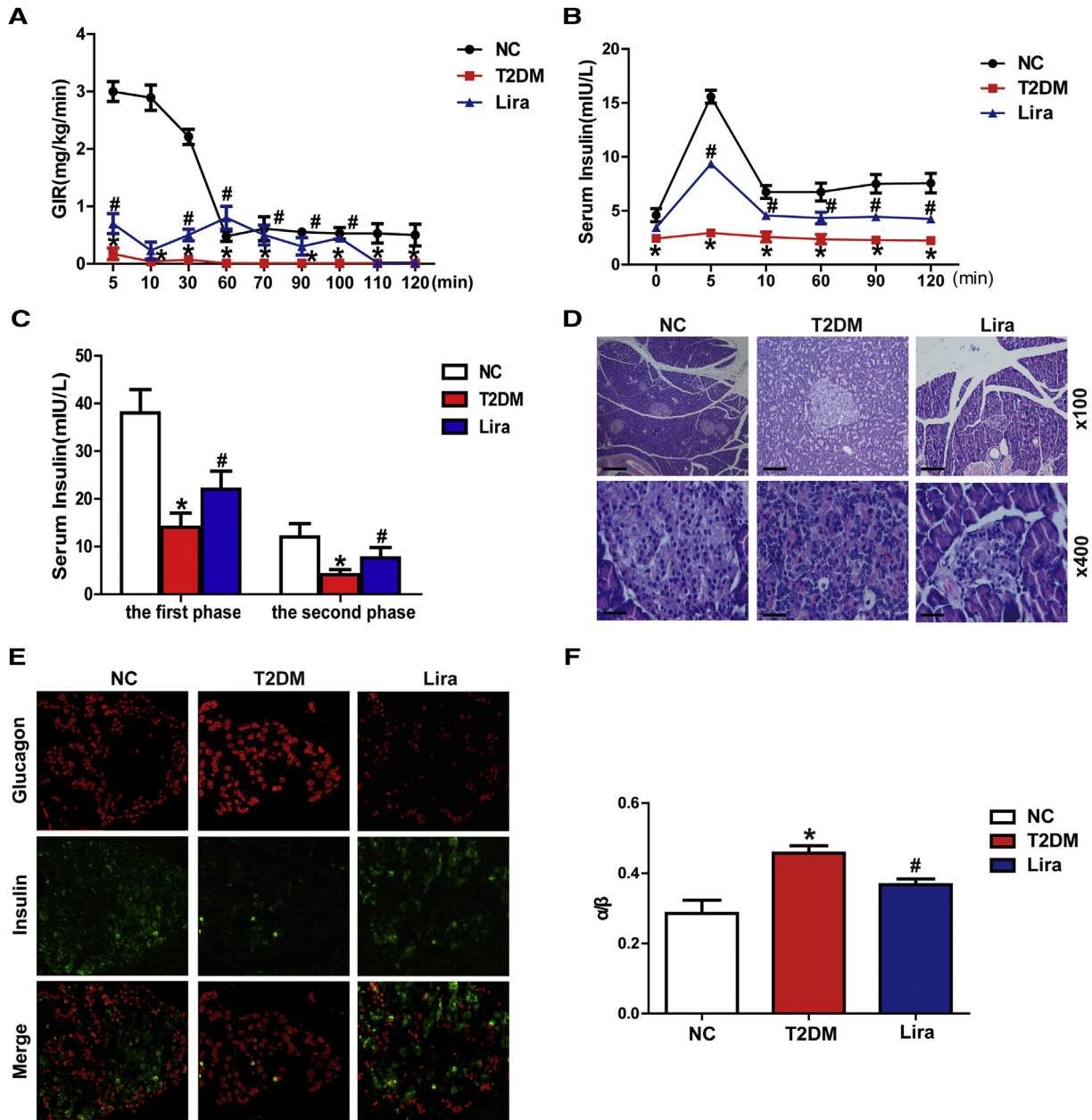


Fig. 2. Effects of Liraglutide on pancreatic islet function and morphology.

HG.³⁰ The functional activation of NOX2 led to metabolic dysfunction in the clonal β -cells of normal rats and humans under various conditions. We detected ROS levels in islets from isolated T2DM rats with or without Apocynin administration. We observed that ROS levels increased by 1.6 folds in islets from isolated T2DM rats compared with the control group, which could be mitigated with the liraglutide treatment (Fig. 4B). In addition, Apocynin had the capacity to reduce ROS levels induced by HG and contributed to the positive effect of liraglutide on INS-1 cells (Fig. 4B). Immunohistochemistry and Western blot confirmed that liraglutide led to an increase in NOX2 expression in T2DM rats compared with normal rats (Fig. 4C–D). In vitro, liraglutide also reduced NOX2 expression in INS-1 cells incubated with HG. Furthermore, NOX2 in INS-1 cells cultured in HG was reduced after pretreatment with Apocynin (Fig. 4E). NOX2 in mannitol group was lower than HG group and there was no statistical difference in NOX2 expression among N + G, HG + G, HG + A and HG + A + G groups (Fig. 4E). Next, Annexin V-FITC/PI flow cytometry was adopted to detect cell apoptosis rate. As a result, the apoptosis rate in HG group was significantly

higher than counterpart in normal group. However, pre-treatment with both liraglutide and Apocynin mitigated cell apoptosis rate in the setting of HG (Fig. 4F). To our surprise, the joint application of liraglutide and Apocynin also alleviated cell apoptosis rate, but there was no statistical difference in cell apoptosis rate among HG + G, HG + A and HG + A + G group (Fig. 4F). Overall, liraglutide can reduce cell apoptosis effectively by inhibiting NOX2-derived ROS generation in vivo and in vitro.

3.5. Liraglutide counteracts HG-induced apoptosis of islets and INS-1 cells by inhibiting the activation of the c-Jun N-terminal protein kinase signaling pathway

There was evidence that NOX2-derived ROS mediate FFA-induced dysfunction and apoptosis of β -cells via JNK pathways.³¹ The GLP-1 receptor agonist prevented oxidative stress-mediated apoptosis in human cardiac progenitor cells (CPCs) by interfering with JNK activation.³² Therefore, we speculated that the protective effects of liraglutide on islets and INS-1 cells under HG conditions were associated with phospho-

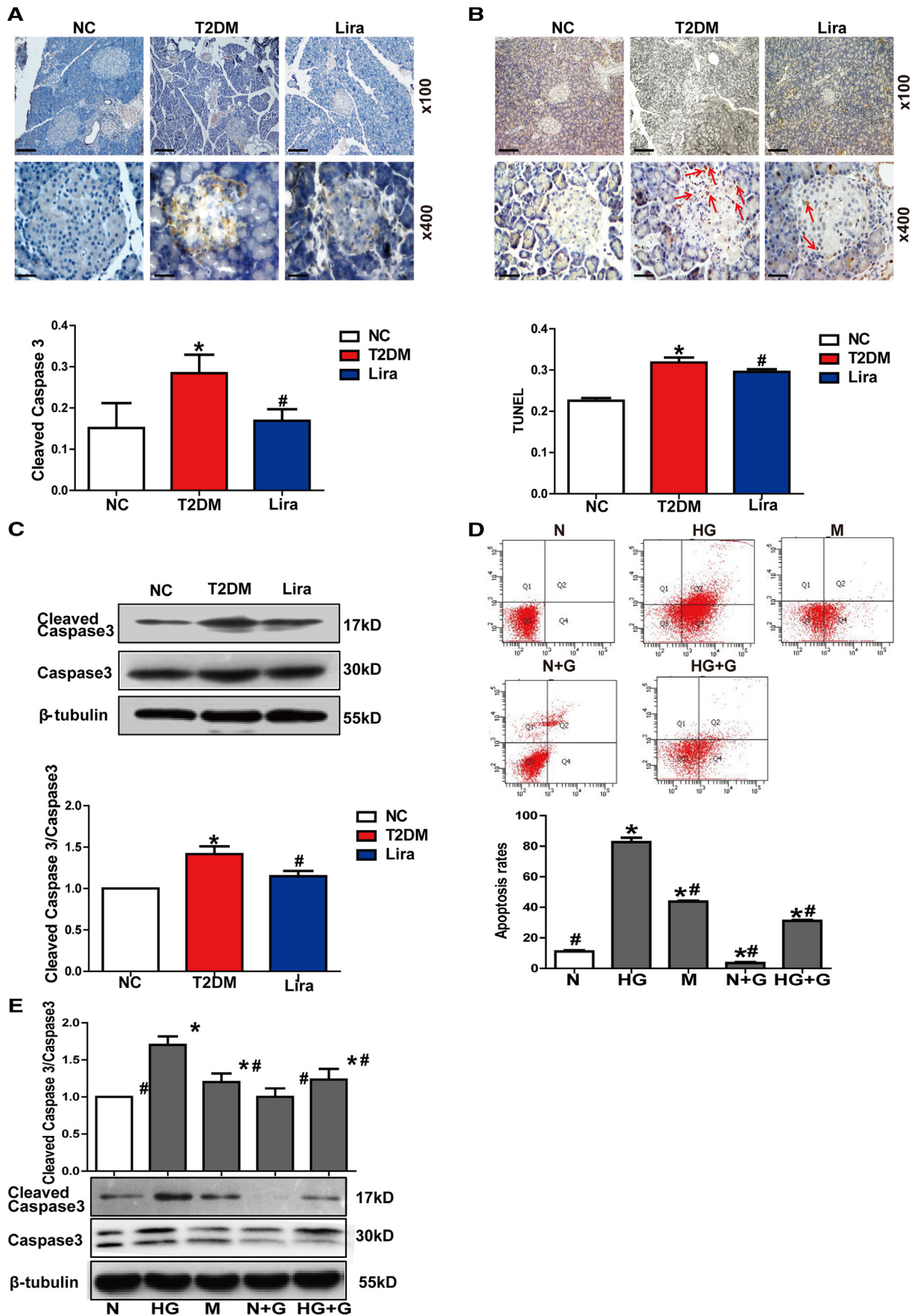


Fig. 3. Liraglutide suppresses HG-induced β -cell apoptosis in vivo and in vitro.

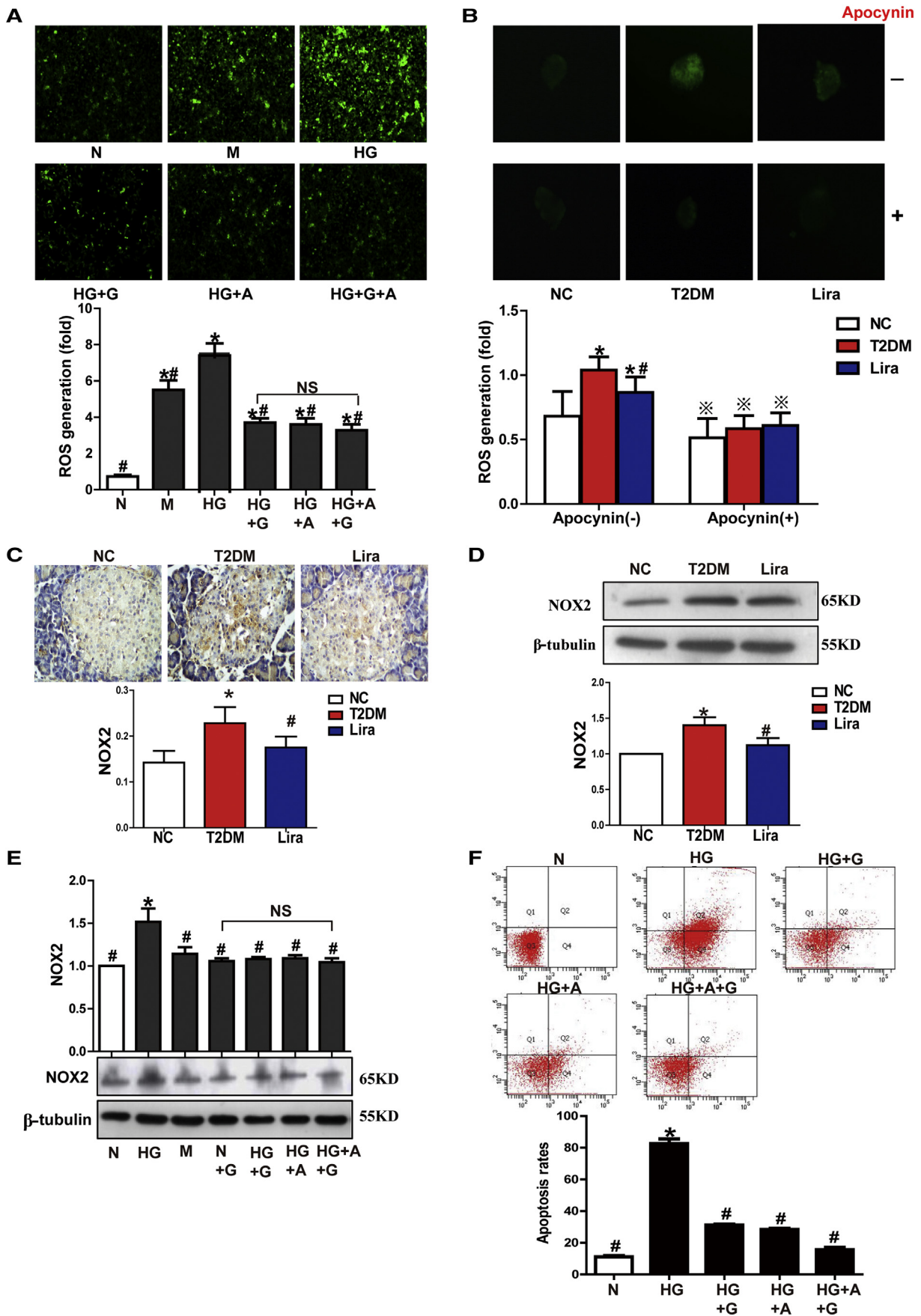


Fig. 4. Liraglutide prevents HG-mediated β -cell apoptosis by inhibiting NOX2-derived ROS generation.

JNK1/2 reduction. As a result, the level of phospho-JNK1/2 in diabetic rats was inhibited by the treatment of liraglutide (Fig. 5A–B). We further validated the effects of GLP-1Ra on JNK signaling pathways. SP600125 is a JNK inhibitor that has been described previously.³³ Treatment or pre-treatment with liraglutide, Apocynin or JNK inhibitor SP600125 (200 μmol/L, 48 h) inhibited the JNK phosphorylation activated by HG both in pancreatic β-cells and in INS-1 cells (Fig. 5C–D). In addition,

we found that the combined application of liraglutide and Apocynin or SP600125 failed to further reduce the JNK phosphorylation levels compared with a single application of the former (Fig. 5C). There was no significant difference in Cleaved Caspase 3/Caspase 3 or the apoptosis rates between the application of JNK inhibitors and the treatment with Apocynin. Cleaved Caspase 3/Caspase 3 and the apoptosis rates showed the same change trends in INS-1 cells, and there were no further

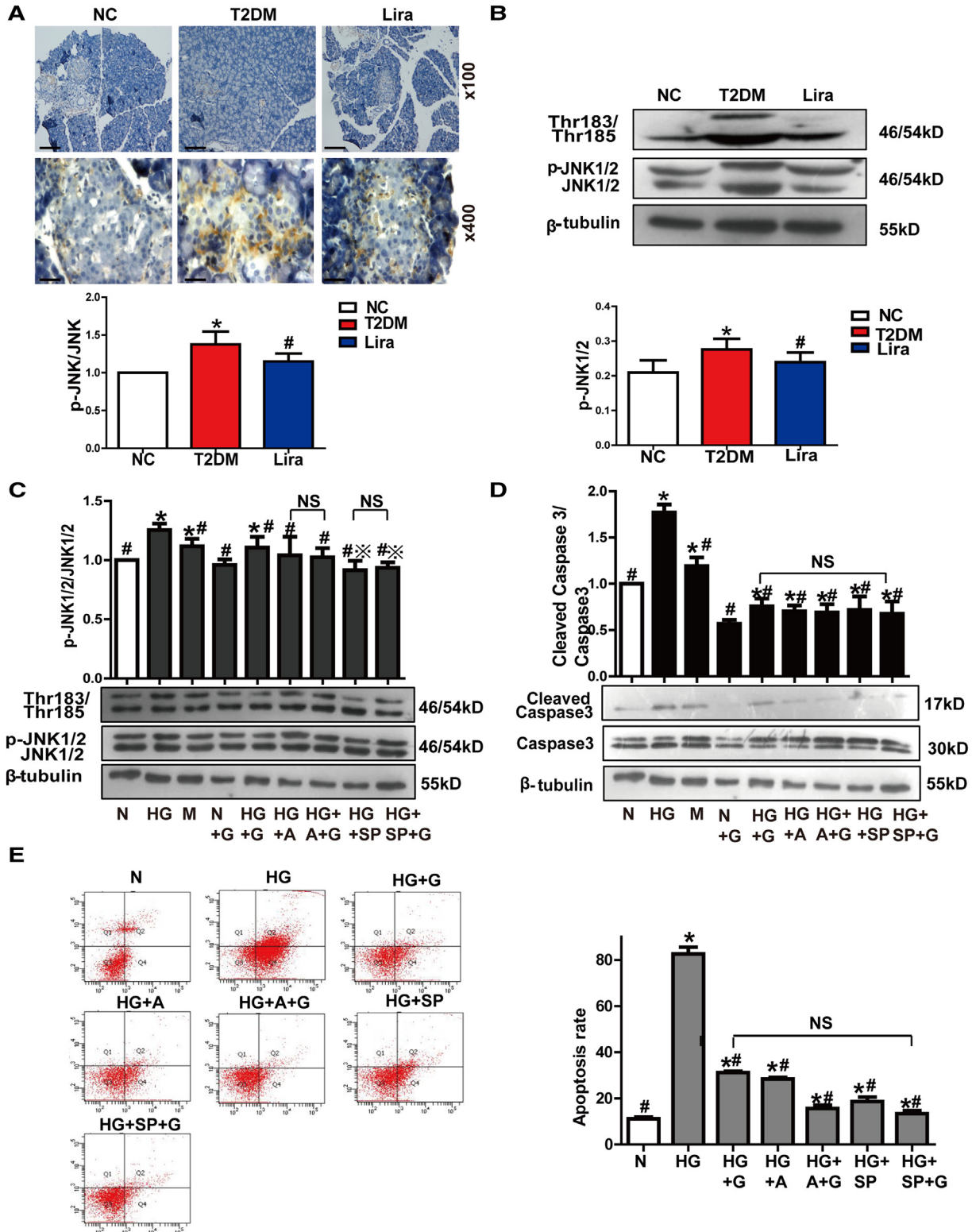


Fig. 5. Liraglutide counteracts HG-induced apoptosis of islets and INS-1 cells by inhibiting the activation of the c-Jun N-terminal protein kinase signaling pathway.

reductions after treatment with liraglutide (Fig. 5D and E). These results indicate that the inhibition of the JNK signaling pathway is responsible for the reduction in HG-induced β -cell apoptosis by inhibiting NOX2-derived ROS generation.

3.6. Liraglutide antagonizes the HG-induced apoptosis of islets and INS-1 cells by promoting the activation of the p-AMPK α signaling pathway

Recently, Magali Balteau reported that the AMPK activated by GLP-1 prevented HG-induced NOX2 activation in adult cardiomyocytes.²⁰ Hence, we hypothesized that the same signaling pathway might exist in pancreatic β -cells and INS-1 cells. As expected, liraglutide inhibited the reduction in the phosphorylation of AMPK α (p-AMPK α) in pancreatic β -cells from diabetic rats and INS-1 cells cultured in HG conditions (Fig. 6A–C). Overall, our data explore a novel mechanism that GLP-1Ra serving as a potential drug alleviates apoptosis in islet cells by NOX2 signaling pathway, which demonstrates that NOX2 can be a therapeutic target of T2DM.

4. Discussion

In the current study, we identify a mechanism by which liraglutide inhibits NOX2 expression to alleviate HG-induced β -cell apoptosis by upregulating AMPK α phosphorylation and downregulating JNK1/2 phosphorylation in vivo and in vitro. This study further supports the notion that GLP-1Ra can act as a promising therapeutic for delaying the progression of DM.

Liraglutide has been clinically licensed as an anti-diabetic agent. It is widely known that GLP-1 acts as an intestinal-derived hormone in vivo and can reduce blood glucose levels mainly by increasing the level of circulating insulin in a glucose-dependent manner.³⁴ In addition to its glucose-lowering properties, GLP-1 exerted protective effects on pancreatic β -cells as well.³⁵ For example, GLP-1 is capable of stimulating pancreatic cell proliferation and β -cells differentiation in the rodent pancreas.³⁶ In this study, liraglutide was found to inhibit pancreatic β -cell apoptosis in diabetic rats and INS-1 cells in HG conditions. Additionally, liraglutide improved islet function and morphology in a STZ/HFD-induced T2DM rat model, consistent with a report showing that GLP-1 added to freshly isolated human islets preserves cell morphology and function and inhibits cell apoptosis.³⁷ In addition, the decreased death rate of INS-1 cells was mainly due to the alleviation of cellular apoptosis, which was indicated by the significantly decreased expression of the apoptotic marker Cleaved Caspase 3. In support of our findings, a previous study showed that GLP-1 protected β -cells against cytokine-induced apoptosis.³⁸ These findings collectively reveal that liraglutide is able to prevent β -cell apoptosis and improves β -cells function.

It is worth mentioning that the relationship between the NOX2-ROS-JNK signaling pathway and β -cell apoptosis has attracted the attention of number of researchers.³⁹ NOX2, as one of the critical subunits of NOX, induced β -cells injury by promoting ROS production, immune responses, and apoptosis.³⁰ Physiological levels of intracellular ROS play a critical role in maintaining cellular homeostasis, whereas excessive ROS generation may speed up the pathophysiological progression of many diseases, including diabetes mellitus. This is consistent with research

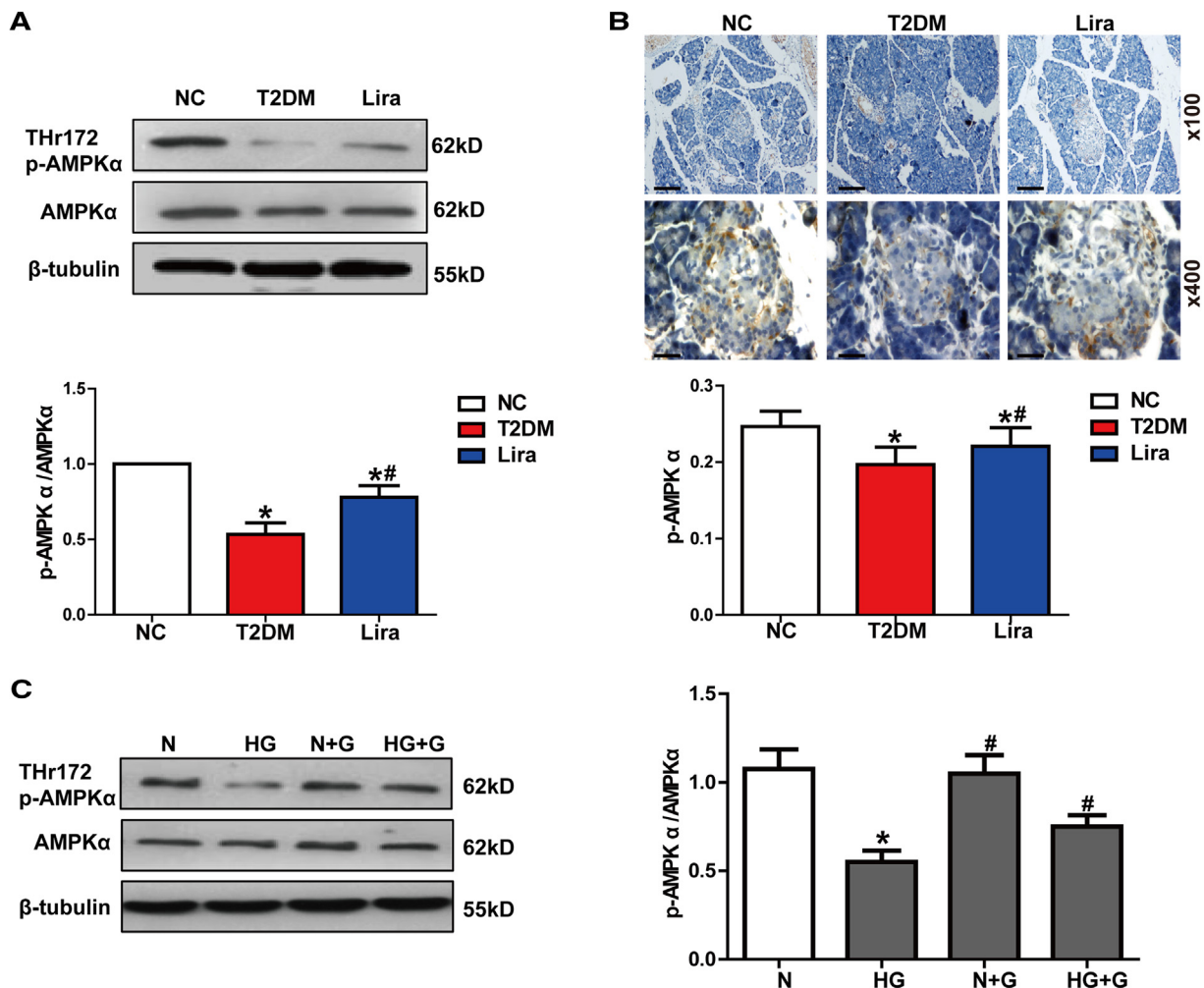


Fig. 6. Liraglutide antagonizes the HG-induced apoptosis of islets and INS-1 cells by promoting the activation of the p-AMPK α signaling pathway.

showing that ROS-mediated mitochondrial dysfunction led to pancreatic β -cell apoptosis.⁴⁰ Furthermore, liraglutide prevented human CPCs from oxidative stress-mediated apoptosis.³² On the basis of the discussion above, we made a hypothesis that inhibiting the NOX2 pathway might serve as an important mechanism for the protective effects of liraglutide on pancreatic β -cells. Our study validated the idea that liraglutide inhibited the increased NOX2 and ROS expression induced by HG *in vivo* and *in vitro*. Furthermore, Apocynin, a NOX2 inhibitor, reversed the impact of HG on NOX2, ROS expression and β -cell apoptosis.

The cJun-N-terminal kinases, JNKs, are members of the mitogen-activated protein kinase (MAPK) family. JNKs were more potently induced in response to cellular stress than to mitogens.⁴¹ JNKs, which consist of three JNK isoforms encoded by three different genes (JNK1, JNK2, JNK3), play a central role in the cellular response to stress, and JNK activity in different cell types is implicated in the pathogenesis of obesity-driven insulin resistance. Stress-activated JNK activation is responsible for Caspase3 activation.⁴² Significant crosstalk between ROS and JNK1/2 was reported in mesangial cells in diabetic rats.⁴³ Syed et al. revealed that the accelerated Rac1-NOX-ROS-JNK1/2 pathway resulted from islet β -cells mitochondrial dysfunction in diabetes *in vivo* and *in vitro*.⁴⁴ Intriguingly, GLP-1Ra prevented oxidative stress-mediated apoptosis in human CPCs by interfering with JNK activation.³² Thus, we infer that liraglutide may alleviate β -cell apoptosis by antagonizing the NOX-ROS-JNK1/2 pathway. As a result, we found that liraglutide decreased the phosphorylation of JNK1/2 by downregulating the expression of NOX2. Cleaved Caspase3 expression decreased without significant differences in pancreatic β -cells and HG induced β -cells with the treatment of liraglutide, Apocynin and JNK inhibitor SP600125, which blocked JNK phosphorylation. This finding not only the first to show the role of NOX-ROS-JNK1/2 pathway regulation in apoptosis in pancreatic islet β -cells but also suggest a brand-new mechanism that is different from increasing the activity of the Igf-2/Igf-1 receptor autocrine loop, which might account for GLP-1-ameliorated islet β -cells injury.³⁸

The upstream molecules and mechanisms responsible for the inhibitory effect of GLP-1 on NOX2 expression remain elusive in diabetes. AMP-activated protein kinase (AMPK), known as a sensor and a master of the cellular energy balance, played an important role in glucose metabolism.⁴⁴ We observed that liraglutide upregulated the phosphorylation of AMPK α under HG conditions to alleviate β -cell apoptosis both *in vivo* and *in vitro*. In support of our finding, previous studies showed that liraglutide protected β -cells from glucolipotoxicity-induced apoptosis by activating the AMPK/mTOR/P70S6K signaling pathway.⁴⁵ A recent study demonstrates that the activation of AMPK α antagonized homocysteine-induced apoptosis in osteocytic MLO-Y4 by regulating the expression of NADPH oxidase 1 (NOX1) and NOX2.⁴⁶ In addition, Baiteau et al. revealed that α 2-AMPK activated by GLP-1 prevents NOX2 activation induced by hyperglycemia in adult cardiomyocytes.²⁰ Therefore, we speculated that AMPK α increased by liraglutide may regulate NOX2/JNK1/2 expression to lessen apoptosis in islet β -cells. As a result, our findings indicate that liraglutide decreases NOX2 expression to prevent β -cell apoptosis by increasing the levels of AMPK α phosphorylation. Altogether, our findings indicate that liraglutide plays a protective role in pancreatic islet β -cells through the p-AMPK α /NOX2/JNK1/2 signaling pathway.

5. Conclusions

In summary, our study demonstrates that liraglutide increases p-AMPK α expression and reduces NOX2-mediated JNK1/2 expression to alleviate HG-induced pancreatic β -cell apoptosis. This suggests that the p-AMPK α /NOX2/JNK1/2 signaling pathway is essential for liraglutide to alleviate HG-induced β -cell apoptosis, which provides a novel mechanism supporting incretin mimetics as promising therapeutics for HG-induced β -cell apoptosis.

Finding

This work was supported by grants from the National Natural Science Foundation of China No. 81300663 (to CJL) and the Science and Technology Funds of Tianjin Municipal Bureau No. 2015KZ092 (to DM).

Acknowledgements

Chun-Jun Li and De-Min Yu contributed to the study design, the data acquisition and interpretation. Min Ding and Qian-Hua Fang performed the experiments and wrote the manuscript. Yuan-Tao Cui, Qi-Ling Shen, Qian Liu and Peng-Hua Wang participated in the work. All authors read and approved the final manuscript and declare no competing financial interests.

References

- Weir GC, Bonner-Weir S. Five stages of evolving beta-cell dysfunction during progression to diabetes. *Diabetes* 2004;53:S16-21.
- Hu F, Qiu X, Bu S. Pancreatic islet dysfunction in type 2 diabetes mellitus. *Arch Physiol Biochem* 2018;6:1-7.
- Andersson LE, Shcherbina L, Al-Majdoub M, et al. Glutamine-elicited secretion of glucagon-like peptide 1 is governed by an activated glutamate dehydrogenase. *Diabetes* 2018;67:372-84.
- Villanueva-Penacarrillo ML, Puente J, Redondo A, Clemente F, Valverde I. Effect of GLP-1 treatment on GLUT2 and GLUT4 expression in type 1 and type 2 rat diabetic models. *Endocrine* 2001;15:241-8.
- Holst JJ, Orskov C, Nielsen OV, Schwartz TW. Truncated glucagon-like peptide 1, an insulin-releasing hormone from the distal gut. *FEBS Lett* 1987;211:169-74.
- Sano H, Terasaki J, Mishiba Y, Imagawa A, Hanafusa T. Exendin-4, a glucagon-like peptide-1 receptor agonist, suppresses pancreatic beta-cell destruction induced by encephalomyocarditis virus. *Biochem Biophys Res Commun* 2011;404:756-61.
- Prigeon RL, Quddusi S, Paty B, D'Alessio DA. Suppression of glucose production by GLP-1 independent of islet hormones: a novel extrapancreatic effect. *Am J Physiol Endocrinol Metab* 2003;285:E701-7.
- Zander M, Madsbad S, Madsen JL, Holst JJ. Effect of 6-week course of glucagon-like peptide 1 on glycaemic control, insulin sensitivity, and beta-cell function in type 2 diabetes: a parallel-group study. *Lancet* 2002;359:824-30.
- Kimura T, Obata A, Shimoda M, et al. Durability of protective effect of dulaglutide on pancreatic β -cells in diabetic mice: GLP-1 receptor expression is not reduced despite long-term dulaglutide exposure. *Diabetes Metab* 2018;44:250-60.
- Brownlee M. The pathobiology of diabetic complications: a unifying mechanism. *Diabetes* 2005;54:1615-25.
- Cheng G, Cao Z, Xu X, van Meir EG, Lambeth JD. Homologs of gp91phox: cloning and tissue expression of Nox3, Nox4, and Nox5. *Gene* 2001;269:131-40.
- Mathews CE, Suarez-Pinzon W, Baust JJ, Strynadka K, Leiter E, Rabinovitch A. Mechanisms underlying resistance of pancreatic islets from ALR/Lt mice to cytokine-induced destruction. *J Immunol* 2005;175:1248-56.
- Newsholme P, Morgan D, Rebelato E, et al. Insights into the critical role of NADPH oxidase(s) in the normal and dysregulated pancreatic beta cell. *Diabetologia* 2009;52:2489-98.
- Wang X, Elksnis A, Wikström P, et al. The novel NADPH oxidase 4 selective inhibitor GLX7013114 counteracts human islet cell death *in vitro*. *PLoS One* 2018;13, e0204271.
- Violi F, Pignatelli P, Pignata C, et al. Reduced atherosclerotic burden in subjects with genetically determined low oxidative stress. *Arterioscler Thromb Vasc Biol* 2013;33:406-12.
- Shan Q, Zhuang J, Zheng G, Zhang Z, Zhang Y, Lu J, et al. Troxerutin reduces kidney damage against BDE-47-induced apoptosis via inhibiting NOX2 activity and increasing Nrf2 activity. *Oxidative Med Cell Longev* 2017;2017:12-2850. 6034692.
- Chandrashekar V, Seth RK, Dattaray D, et al. HMGB1-RAGE pathway drives peroxynitrite signaling-induced IBD-like inflammation in murine nonalcoholic fatty liver disease. *Redox Biol* 2017;13:8-19.
- Li N, Li B, Brun T, et al. NADPH oxidase NOX2 defines a new antagonistic role for reactive oxygen species and cAMP/PKA in the regulation of insulin secretion. *Diabetes* 2012;61:2842-50.
- Syed I, Kyathanahalli CN, Jayaram B, et al. Increased phagocyte-like NADPH oxidase and ROS generation in type 2 diabetic ZDF rat and human islets: role of Rac1-JNK1/2 signaling pathway in mitochondrial dysregulation in the diabetic islet. *Diabetes* 2011;60:2843-52.
- Baiteau M, Van Steenberg A, Timmermans AD, et al. AMPK activation by glucagon-like peptide-1 prevents NADPH oxidase activation induced by hyperglycemia in adult cardiomyocytes. *Am J Physiol Heart Circ Physiol* 2014;307:H1120-33.
- Kim JY, Lim DM, Moon CI, et al. Exendin-4 protects oxidative stress-induced beta-cell apoptosis through reduced JNK and GSK3 beta activity. *J Korean Med Sci* 2010;25:1626-32.
- Cummings BP, Stanhope KL, Graham JL, et al. Chronic administration of the glucagon-like peptide-1 analog, liraglutide, delays the onset of diabetes and lowers triglycerides in UCD-T2DM rats. *Diabetes* 2010;59:2653-61.

23. Phelps EA, Cianciarusi C, Michael IP, et al. Aberrant accumulation of the diabetes autoantigen GAD65 in Golgi membranes in conditions of ER stress and autoimmunity. *Diabetes* 2016;65:2686–99.
24. Li CJ, Sun B, Fang QH, et al. Saxagliptin induces β -cell proliferation through increasing stromal cell-derived factor-1 α in vivo and in vitro. *Front Endocrinol (Lausanne)* 2017;8:326.
25. Wu YJ, Guo X, Li CJ, et al. Dipeptidyl peptidase-4 inhibitor, vildagliptin, inhibits pancreatic beta cell apoptosis in association with its effects suppressing endoplasmic reticulum stress in db/db mice. *Metab Clin Exp* 2015;64:226–35.
26. Kirk RK, Pyke C, von Herrath MG, et al. Immunohistochemical assessment of glucagon-like peptide 1 receptor (GLP-1R) expression in the pancreas of patients with type 2 diabetes. *Diabetes Obes Metab* 2017;19:705–12.
27. Xiong Y, Yepuri G, Necetin S, Montani JP, Ming XF, Yang Z. Arginase-II promotes tumor necrosis factor-alpha release from pancreatic acinar cells causing beta-cell apoptosis in aging. *Diabetes* 2017;66:1636–49.
28. Qin H, Lee IF, Panagiotopoulos C, et al. Natural killer cells from children with type 1 diabetes have defects in NKG2D-dependent function and signaling. *Diabetes* 2011;60:857–66.
29. Shadel GS, Horvath TL. Mitochondrial ROS signaling in organismal homeostasis. *Cell* 2015;163:560–9.
30. Mohammed AM, Kowluru A. Activation of apocynin-sensitive NADPH oxidase (Nox2) activity in INS-1 832/13 cells under glucotoxic conditions. *Islets* 2013;5:129–31.
31. Yuan H, Zhang X, Huang X, et al. NADPH oxidase 2-derived reactive oxygen species mediate FFAs-induced dysfunction and apoptosis of beta-cells via JNK, p38 MAPK and p53 pathways. *PLoS One* 2010;5, e15726.
32. Laviola L, Leonardini A, Melchiorre M, et al. Glucagon-like peptide-1 counteracts oxidative stress-dependent apoptosis of human cardiac progenitor cells by inhibiting the activation of the c-Jun N-terminal protein kinase signaling pathway. *Endocrinology* 2012;153:5770–81.
33. Vella RE, Pillon NJ, Zarrouk B, et al. Ozone exposure triggers insulin resistance through muscle c-Jun N-terminal kinase activation. *Diabetes* 2015;64:1011–24.
34. Parkes DG, Pittner R, Jodka C, Smith P, Young A. Insulinotropic actions of exendin-4 and glucagon-like peptide-1 in vivo and in vitro. *Metabolism* 2001;50:583–9.
35. Lee YS, Jun HS. Anti-diabetic actions of glucagon-like peptide-1 on pancreatic beta-cells. *Metab Clin Exp* 2014;63:9–19.
36. Perfetti R, Zhou J, Doyle ME, Egan JM. Glucagon-like peptide-1 induces cell proliferation and pancreatic-duodenum homeobox-1 expression and increases endocrine cell mass in the pancreas of old, glucose-intolerant rats. *Endocrinology* 2000;141:4600–5.
37. Farilla L, Bulotta A, Hirshberg B, et al. Glucagon-like peptide 1 inhibits cell apoptosis and improves glucose responsiveness of freshly isolated human islets. *Endocrinology* 2003;144:5149–58.
38. Cornu M, Yang JY, Jaccard E, Poussin C, Widmann C, Thorens B. Glucagon-like peptide-1 protects beta-cells against apoptosis by increasing the activity of an IGF-2/IGF-1 receptor autocrine loop. *Diabetes* 2009;58:1816–25.
39. Helmcke I, Heumüller S, Tikkanen R, Schröder K, Brandes RP. Identification of structural elements in Nox1 and Nox4 controlling localization and activity. *Antioxid Redox Signal* 2009;11:1279–87.
40. Liu C, Fu Y, Li CE, Chen TA-O, Li X. Phycocyanin-functionalized selenium nanoparticles reverse palmitic acid-induced pancreatic beta cell apoptosis by enhancing cellular uptake and blocking reactive oxygen species (ROS)-mediated mitochondria dysfunction. *J Agric Food Chem* 2017;65:4405–13.
41. Chang L, Karin M. Mammalian MAP kinase signalling cascades. *Nature* 2001;410:37–40.
42. Kim BC, Hg K, Lee SA, et al. Genipin-induced apoptosis in hepatoma cells is mediated by reactive oxygen species/c-Jun NH2-terminal kinase-dependent activation of mitochondrial pathway. *Biochem Pharmacol* 2005;70:1398–407.
43. Ohashi N, Urushihara M, Satou R, Kobori H. Glomerular angiotensinogen is induced in mesangial cells in diabetic rats via reactive oxygen species – ERK/JNK pathways. *Hypertens Res* 2010;33:1174–81.
44. Angin Y, Beauloye C, Horman S, et al. Regulation of carbohydrate metabolism, lipid metabolism, and protein metabolism by AMPK. *EXS* 2016;107:23–43.
45. Miao XY, Gu ZY, Liu P, Hu Y, Li L, Gong YP, et al. The human glucagon-like peptide-1 analogue liraglutide regulates pancreatic beta-cell proliferation and apoptosis via an AMPK/mTOR/P70S6K signaling pathway. *Peptides* 2013;39:71–9.
46. Takeno A, Kanazawa I, Tanaka K, et al. Activation of AMP-activated protein kinase protects against homocysteine-induced apoptosis of osteocytic MLO-Y4 cells by regulating the expressions of NADPH oxidase 1 (Nox1) and Nox2. *Bone* 2015;77:135–41.